Journal of the Iranian Chemical Society
https://doi.org/10.1007/s13738-019-01776-2

ORIGINAL PAPER

Synthesis and characterization of 2-benzylidene-1,3-indandione derivatives as in vitro quantification of amyloid fibrils

Hadi Adibi[1] · Maryam Mehrabi[2] · Kazhal Amiri[3] · Saeed Balalaie[4,5] · Reza Khodarahmi[5,6]

Received: 19 February 2019 / Accepted: 30 August 2019

Abstract

Timely detection of amyloid aggregations has a critical role in the treatment of degenerative nervous system disorders such as Alzheimer's, Parkinson's disease and systemic amyloidosis. Thioflavin T (ThT) is a dye considered for the detection of amyloids. However, ThT cannot cross the blood–barrier barrier due to positive charge and low lipophilicity. In the present study, a variety of 2-benzylidene-1,3-indandione derivatives **5a**–**5j** were synthesized as neutral fluorescence probe candidates for identification of amyloid. Among these compounds, only compound 2-(2-hydroxybenzylidene)-1,3-indandione 5a was selected for further examination, because its fluorescence intensity showed the significant increasing upon interaction with amyloid aggregates. The compound **5a** was compared to standard and conventional probe such as ThT. The compound **5a** was excited at its specified wavelength, and the fluorescence emission signal was recorded in the presence of different concentrations of the protein/peptide (amyloid aggregated and native protein). According to the obtained results, it can be seen that 2-(2-hydroxybenzylidene)-1,3-indandione **5a** selectively and specifically bind to amyloid fibrils, such as ThT. Due to the neutrality of electrical charge and high lipophilicity coefficient of the synthesized compound **5a**, it is possible for it to cross from the blood–brain barrier. Our results show that this synthetic derivative can be considered as a suitable probe to detect in vitro amyloid aggregations.

Keywords Amyloid aggregation · Alzheimer's disease (AD) · Indanone derivatives · Thioflavin T (ThT) · β-Amyloid plaques

Introduction

Fibrillar protein aggregates are a major cause of amyloidosis, a group of diseases created by self-aggregation of some normal proteins into harmful filamentous deposits (amyloid fibrils). Amyloid fibrils are correlated with the most neurodegenerative disorder, such as Alzheimer's, Parkinson's, and systemic amyloidosis [1]. For example, Alzheimer's disease (AD) is a type of degenerative nervous system disorders that gradually declines the mental abilities of the patient [2, 3]. Amyloid-beta (Aβ) and Tau are the two major proteins extensively involved in the AD pathology. Both proteins convert from innocuous soluble forms to cytotoxic oligomers [4] and fibers (with cross-β-sheet structure) [5]. There are great interests about the pathological process of Tau aggregation, because Tau deposition more occur in the temporal lobe of the brain and it is a better predictor of AD than Aβ deposition that happen in any region of the brain [6]. This intrinsically disordered protein consists of three or four repeated regions with similar amino acid sequences. Recently, studies have demonstrated

✉ Reza Khodarahmi
rkhodarahmi@kums.ac.ir; rkhodarahmi@mbrc.ac.ir

[1] Pharmaceutical Sciences Research Center, Health Institute, Kermanshah University of Medical Sciences, Kermanshah, Iran

[2] Department of Biology, Faculty of Sciences, Razi University, Kermanshah, Iran

[3] Student Research Committee, Kermanshah University of Medical Sciences, Kermanshah, Iran

[4] Peptide Chemistry Research Center, K. N. Toosi University of Technology, P.O. Box 15875-4416, Tehran, Iran

[5] Medical Biology Research Center, Health Technology Institute, Kermanshah University of Medical Sciences, Kermanshah, Iran

[6] Pharmacognosy and Biotechnology Department, Faculty of Pharmacy, Kermanshah University of Medical Sciences, Kermanshah, Iran

Published online: 20 September 2019

that only a small part of the Tau molecule is contributed in the aggregation process [5]. In Tau polymerization, the formation of β-sheet structure is attributed to two hydrophobic short hexapeptide motifs in the second and third repeat of Tau, PHF6*^{275}VQIINK^{280}(in R2) and PHF6^{306}VQIVYK^{311}(inR3), and it has been verified that the interaction between these two regions causes to the unique PHF structure [7]. In our previous study, we synthesized a modified PHF6 heptapeptide (FVQIVYH) and amyloid fibril formation by tau protein and the modified PHF6 heptapeptide (FVQIVYH) were verified through some specific methods of amyloid detection (ThT fluorescence, XRD, far UV-CD and AFM). This modified PHF6 heptapeptide (FVQIVYH) is known as FV peptide [8].

The greater we understand amyloidosis molecular details, the greater we can control amyloid formation and consequently, neurodegenerative diseases. This requires a reliable probe for identifying amyloids. Detection of amyloid formation is carried out in a variety of ways, including iodine colorimetric method, crystalline violet staining, optical dispersion, Congo red (CR), transmission electron microscopy (TEM), atomic force microscopy (AFM), thioflavin S (ThS), and thioflavin T (ThT) [9]. ThT, in the form of dimer, hexamer and micelle, has the ability to interact with amyloid. Its structure is two-ring of benzothiazole and benzylamine; these two rings have the ability to rotate freely around their shared carbon–carbon bond in aqueous media that rapidly quenches excited states generated by photon excitation. This rotation is limited when ThT bind to amyloid fibrils, so it exhibits fluorescence properties [10–12]. ThT is not able to pass through the cell membrane due to the ThT positive charge, so it is not suitable for the study of amyloid aggregation in the cell [13]. In addition, compounds without a net positive charge can mainly cross the blood–brain barrier (BBB) [14].

In the current study, with the purpose of producing such compounds, a variety of 2-benzylidene-1,3-indandione derivatives were synthesized as markers for identification of amyloid (Scheme 1). Among them, 2-(2-hydroxybenzylidene)-1,3-indandione **5a** has been found neutral ThT analog fluorescence probe, and it employed to determine quantitatively the amyloid fibrils comparison with conventional methods. The resulting data may be useful in providing mechanistic insights to develop potential diagnostic, curative, and/or preventive strategies in vivo against amyloid-related neurodegenerative disorders.

Materials and methods

Chemicals and equipments

Acetone, bovine serum albumin (BSA), Congo red (CR) and ThT were provided by Sigma (St. Louis, MO, USA.). The chemical compounds were purchased from Merck chemicals (Darmstadt, Germany). All solutions were prepared by sterilizing double distilled water. The structure of compounds was characterized by IR, ^{1}H-NMR spectra and mass spectrometry (MS). IR spectrum was recorded on a Shimadzu 470 spectrophotometer (KBr disk). 1H-NMR spectrum was recorded on a Bruker FT-250 NMR spectrophotometer using DMSO-*d*6 as solvent and tetramethylsilane (TMS) as an internal standard. The MS analysis was performed using a MS system comprising a Finnegan MAT Spectra System P4000 pump coupled with a UV6000LP diode array detector and a Finnigan AQA mass spectrometer. A Cary 100 Bio (Varian) spectrophotometer was used for protein determination. All fluorescence measurements were performed in the ratio mode using a 1-cm cell in a Cary Eclipse (Varian) fluorescence spectrophotometer, equipped with a 150 W xenon lamp and a thermostatic cell holder, at room temperature or as stated. Appropriate vehicle controls were run in all experiments. All the reported results are averages of 2–3 separate experiments whenever the coefficients of variation were less than 5%. Other devices used in this study were pH/EC Meter (Wm-50EG) (Dkktoad) and Heater/Stirrer RH basic 2 (IKA®).

Synthesis of 2-benzylidene-1,3-indandione derivatives 5a–5j

In a round-bottomed flask (25 ml), 1,3-indandione (1 mmol, 0.146 g), benzaldehyde derivatives (1 mmol), pyridine (100 µl) and ethanol (5 ml) were stirred under reflux conditions for 2–3 h. After the reaction was completed (TLC analysis), the reaction mixture was allowed to stand at room temperature for the next 12 h and then the cold distilled water was added to the solution and the precipitate was filtered, washed with *n*-hexane and distilled water, crystallized with appropriate solvent and dried to afford the corresponding; compounds **5a**–**5j** were obtained in % 92–99 yields (Scheme 1; Table 1) [15, 16]. Structural assignments of the products are based on their IR, 1H-NMR, MS and melting point.

2-(2-Hydroxybenzylidene)-1*H*-indene-1,3(2*H*)-dione (compound 5a)

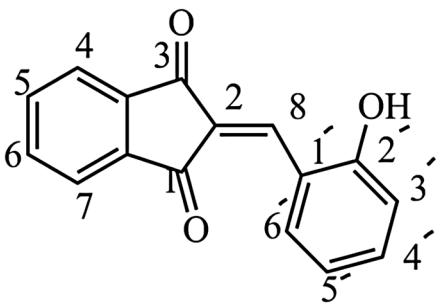

M.W. = 250. 2; m.p. = 196 °C; color: Orange; **FT-IR (KBr, cm^{-1})**: $\bar{\upsilon}$ 3147 (stretch, CH_{Arom}), 2939 (stretch, $CH_{Aliphatic}$),

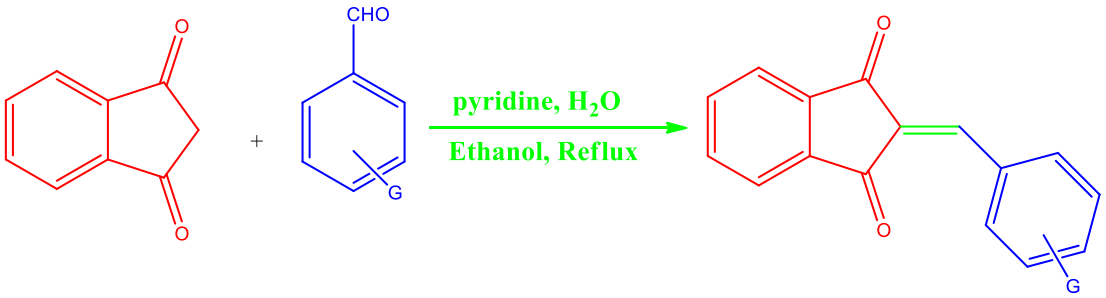

G = Hydroxy, Dihydroxy, Trihydroxy, Isopropyl, **5a-5j**

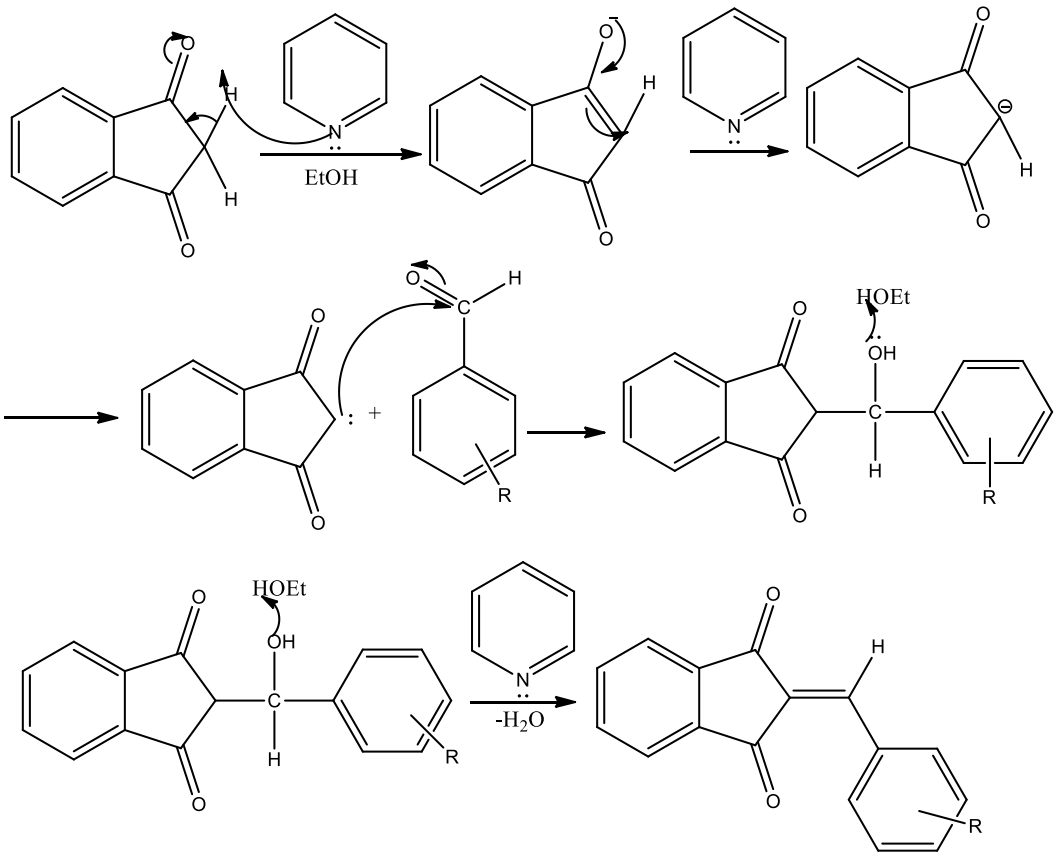

Scheme 1 The synthesis of 2-benzylidene-1,3-indandione compounds: reaction conditions and the mechanism

Table 1 The synthesized compounds

Compound	Name	Yield (%)	Excitation wavelength (nm)
5a	2-(2-Hydroxybenzylidene)-1*H*-indene-1,3(2*H*)-dione	98	320
5b	2-(3-Hydroxybenzylidene)-1*H*-indene-1,3(2*H*)-dione	98	390
5c	2-(4-Hydroxybenzylidene)-1*H*-indene-1,3(2*H*)-dione	97	400
5d	2-(2,3-Dihydroxybenzaldehyde)-1*H*-indene-1,3(2*H*)-dione	97	400
5e	2-(2,4-Dihydroxybenzaldehyde)-1*H*-indene-1,3(2*H*)-dione	99	300
5f	2-(2,5-Dihydroxybenzaldehyde)-1*H*-indene-1,3(2*H*)-dione	94	400
5 g	2-(3,4-Dihydroxybenzaldehyde)-1*H*-indene-1,3(2*H*)-dione	94	400
5 h	2-(2-Hydroxy-3-methoxybenzaldehyde)-1*H*-indene-1,3(2*H*)-dione	96	360
5i	2-(4-Hydroxy-3-methoxybenzaldehyde)-1*H*-indene-1,3(2*H*)-dione	95	420
5j	2-(4-Isopropylbenzaldehyde)-1*H*-indene-1,3(2*H*)-dione	92	370

1712 (stretch, C=O), 1674 (stretch, $C=C_{Vinyl}$), 1570 (stretch, $C=C_{Arom}$), 1462 (stretch, $C=C_{Arom}$), 1276 (stretch, OH_{phenol}), 1215 (stretch, C–O), 1157 (stretch, O–C, 732 (OOP, C–H); **^{1}H–NMR (300 MHz, DMSO-d_6):** δ 10.83 (s, 1H, H_{Phenol}), 8.86 (d, $J=7.9$ Hz, H_4), 8.31 (s, 1H, H_{vinyl}), 7.96 (d, $J=6.35$ Hz, 1H, $H_{6'}$), 7.94 (m, 2H, $H_{4',5'}$), 7.91 (d, $J=6.35$ Hz, 1H, $H_{3'}$), 7.44 (t, $J=7.45$ Hz, 1H, H_6), 6.98 (d, $J=8.2$, 1H, H_7), 6.92 (t, $J=7.55$, 1H, H_5); **Mass (m/z, %):** 252 (M, 122), 233 (M-11, 51.18), 221 (M-21, 5.55), 225 (M-45, 23.31), 114 (M-56, 1.25), 165 (M-85, 25.51), 145 (M-125, 81.14), 125 (M-145, 4.24), 81 (M-161, 51.18), 16 (M-114,4.21), 63 (M-181, 1.11), 52 (M-222, 1.11).

2-(3-Hydroxybenzylidene)-1*H*-indene-1,3(2*H*)-dione (compound 5b)

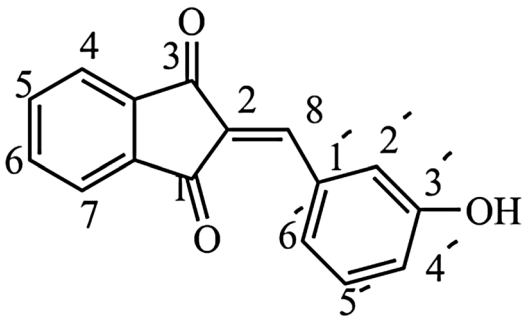

M.W. = 250. 2; m.p. = 221 °C; color: Lemon; **FT–IR (KBr, cm^{-1}):** $\bar{\upsilon}$3741(overtone, C=O), 3240 (stretch, OH), 3024 (stretch, CH_{Arom}), 2924 (stretch, $CH_{Aliphatic}$), 1720 (stretch, C=O), 1666 (stretch, $C=C_{Vinyl}$), 1585 (stretch, $C=C_{Arom}$), 1454 (stretch, $C=C_{Arom}$), 1230 (stretch, C–O), 1180 (stretch, O–C, 1157 (stretch, O–C), 740 (OOP, C–H); **^{1}H-NMR (300 MHz, $CHCl_3$):** δ 8.56 (s, 1H, $H_{2'}$), 8.26 (d, $J=7.5$ Hz, 2H, $H_{4'}$), 8.04 (d, $J=4.45$ Hz, 2H, $H_{4,7}$), 7.85 (d, $J=8.55$ Hz, 2H, $H_{5,6}$), 7.81 (s, 1H, H_{vinyl}), 7.53 (d, $J=7.9$ Hz, 1H, $H_{6'}$), 7.47 (t, $J=7.81$ Hz, 1H, $H_{5'}$)**; Mass (m/z, %):** 250 (M, 37.50), 233 (M-17, 8.34), 165 (M-85, 80), 139 (M-111, 20), 118 (M-132, 3.33), 104 (M-146, 5.55), 89 (M-161, 4.47), 76 (base peak, 100), 63 (M-187, 6.49), 50 (M-200,3.57).

2-(4-Hydroxybenzylidene)-1*H*-indene-1,3(2*H*)-dione (compound 5c)

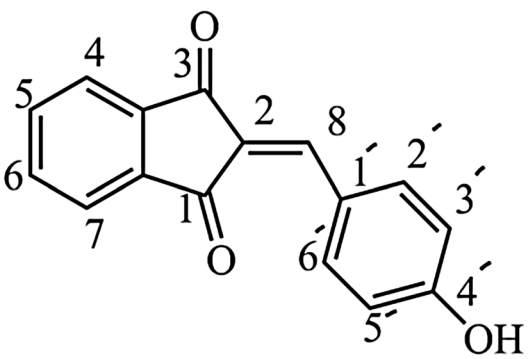

M.W. = 250.2; m.p. = 215 °C; color: Yellow; **FT–IR (KBr, cm^{-1}):** $\bar{\upsilon}$, 3398 (stretch, OH), 3190 (stretch, CH_{Arom}), 2954 (stretch, $CH_{Aliphatic}$), 1708 (stretch, C=O), 1666 (stretch, $C=C_{Vinyl}$), 1566 (stretch, $C=C_{Arom}$), 1477 (stretch, $C=C_{Arom}$), 1257 (stretch, OH_{phenol}), 1207 (stretch, C–O), 1087 (stretch, C–O), 732 (OOP, C–H); **^{1}H–NMR (300 MHz, DMSO-d_6):** δ 10.91 (s, 1H, OH_{Phenol}), 8.52–8.55 (d, 2H, $J=8.7$ Hz, $H_{2',6'}$), 7.88–7.95 (m, 4H, $H_{4,5,6,7}$), 6.93–6.96 (d, 2H, $J=8.4$ Hz, $H_{3',5'}$), 6.2 (s, 1H, H_{Vinyl}); **Mass (m/z, %):** 250 (M, 5.35), 233 (M-17, 18), 194 (M-56, 8.8), 165 (M-85, 7.57), 139 (M-111, 8.14), 118 (M-132, 8.51), 104 (M-146, 57), 89 (M-161, 4.44), 76 (base peak, 100), 63 (M-187, 5.52), 50 (M-200, 1.65).

2-(2,3-Dihydroxybenzaldehyde)-1*H*-indene-1,3(2*H*)-dione (compound 5d)

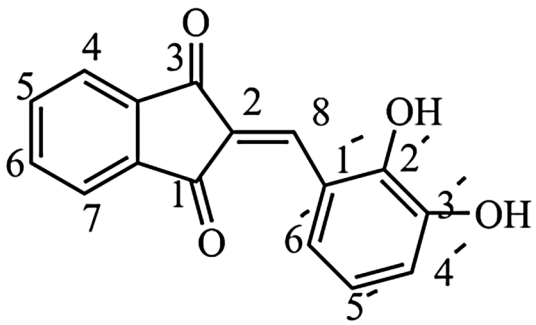

M.W. = 266.2; m.p. = 179 °C; color: Yellow; **FT–IR (KBr, cm^{-1}):** $\bar{\upsilon}$ 3738(overtone, C=O), 3444 (stretch, OH), 3421 (stretch, OH), 3089 (stretch, CH_{Arom}), 2924 (stretch, $CH_{Aliphatic}$), 1708 (stretch, C=O), 1674 (stretch, $C=C_{Vinyl}$), 1570 (stretch, $C=C_{Arom}$), 1473 (stretch, $C=C_{Arom}$), 1273 (stretch, OH_{phenol}), 1215 (stretch, C–O), 1153 (stretch, O–C), 732 (OOP, C–H); **^{1}H–NMR (300 MHz, DMSO-d_6):** δ 10.19 (s, 1H, H_{Phenol}), 8.97–8.98 (d, $J=7.1$ Hz, H_4), 8.58 (s, 1H, H_{vinyl}), 7.95–7.96 (d, $J=5.05$ Hz, 1H, $H_{6'}$), 7. 4 (m, 2H, $H_{4',5'}$), 7.39–7.41 (t, $J=11.45$ Hz, 1H, H_6), 6.94–6.96 (d, $J=7.95$ Hz, 1H, H_7), 6.74–6.77 (t, $J=15.75$ Hz, 1H, H_5); **Mass (m/z, %):** 266 (M, 14), 249 (M-17, 14), 222 (M-44, 11.1), 181 (M-85, 16.2), 165 (M-101, 25.1), 152 (M-114, 28.8), 134 (M-132, 15.5), 104 (M-162, 60.7), 93 (M-173, 29.6), 76 (base peak, 100), 63 (M-203, 44.4), 50 (M-216, 85.1).

2-(2,4-Dihydroxybenzaldehyde)-1*H*-indene-1,3(2*H*)-dione (compound 5e)

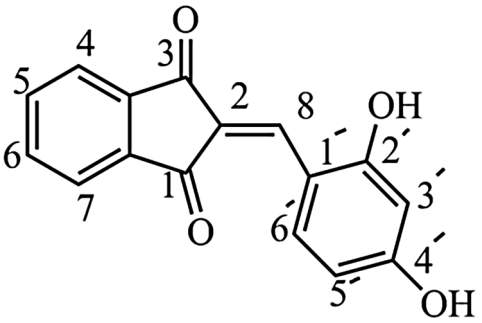

M.W. = 266.2; m.p. = 232.4 °C; color: Brown; **FT–IR (KBr, cm^{-1}):** $\bar{\upsilon}$ 3749(overtone, C=O), 3248 (stretch, OH), 3097 (stretch, CH_{Arom}), 2927 (stretch, $CH_{Aliphatic}$), 1712 (stretch, C=O), 1658 (stretch, $C{=}C_{Vinyl}$), 1554 (stretch, $C{=}C_{Arom}$), 1469 (stretch, $C{=}C_{Arom}$), 1300 (stretch, OH_{phenol}), 1215 (stretch, C–O), 1161 (stretch, O–C), 729 (OOP, C–H); **^{1}H–NMR (300 MHz, DMSO-d_6):** δ 10.95 (s, 1H, H_{Phenol}), 10.80 (s, 1H, H_{Phenol}), 8.95–8.96 (d, J = 7. 95 Hz, 1H, H_4), 8.28 (s, 1H, H_{vinyl}), 8.17–8.19 (d, J = 8.2 Hz, 1H, $H_{6'}$), 7.80 (s, 1H, $H_{3'}$), 7.68–7.71 (t, J = 15.65 Hz, 1H, H_6), 7.51–7.54 (d, J = 8.2 Hz, 1H, H_6'), 6.65–6.67 (d, J = 7.7 Hz, 1H, H_7), 6.40–6.43 (t, J = 15.75, 1H, H_5); **Mass (m/z, %):** 266 (M, 11.8), 246 (M-20, 68.1), 218 (M-48, 25.1), 189 (M-77, 95.5), 163 (M-103, 25.9), 152 (M-114, 8.8), 139 (M-127, 10.3), 113 (M-153, 34.8), 101 (M-165, 9.6), 88 (M-178, 31.1), 63 (M-203, 45.1), 50 (M-216, 63.7).

2-(2,5-Dihydroxybenzaldehyde)-1*H*-indene-1,3(2*H*)-dione (compound 5f)

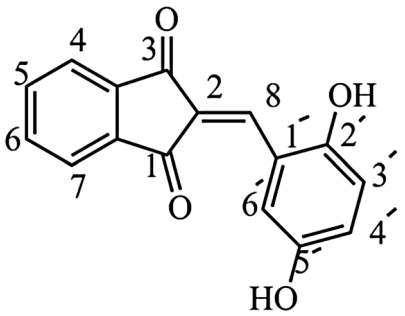

M.W. = 266.2; m.p. = 185 °C; color: Brown**; FT–IR (KBr, cm^{-1}):** $\bar{\upsilon}$ 3738(overtone, C=O), 3414 (stretch, OH), 3109 (stretch, CH_{Arom}), 2912 (stretch, $CH_{Aliphatic}$), 1716 (stretch, C=O), 1685 (stretch, $C{=}C_{Vinyl}$), 1566 (stretch, $C{=}C_{Arom}$), 1458 (stretch, $C{=}C_{Arom}$), 1246 (stretch, OH_{phenol}), 1219 (stretch, C–O), 1157 (stretch, O–C), 740 (OOP, C–H); **^{1}H–NMR (300 MHz, DMSO-d_6):** δ 9.53–9.55 (d, J = 7.15 Hz, 1H, H_4), 8.91 (s, 1H, H_{vinyl}), 8.06–8.09 (t, J = 15.15 Hz, 1H, $H_{6'}$), 8.03–8.04 (d, J = 6.05 Hz, 2H, $H_{3',4'}$), 7.96–7.99 (t, J = 12. 5 Hz, 1H, H_6), 6.85–6.86 (d, J = 8. 1 Hz, 1H, H_7); **Mass (m/z, %):** 274 (M+8,14.8), 266 (M, 3.7), 246 (M-20, 22.2), 189 (M-77, 62.9), 163 (M-103, 18.5), 139 (M-127, 12.5), 114 (M-152, 29.6), 103 (M-162. 26.6), 93 (M-173, 46.6), 76 (M-190, 93.3), 63 (M-203, 44.4), 55 (M-211, 54.8), 43 (M-223, 100).

2-(3,4-Dihydroxybenzaldehyde)-1*H*-indene-1,3(2*H*)-dione (compound 5 g)

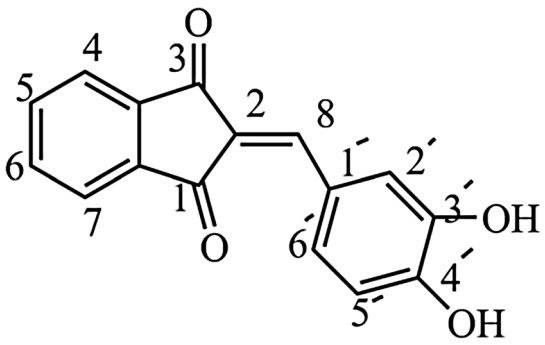

M.W. = 266.2; m.p. = 250 °C; color: Light Green; **FT–IR (KBr, cm^{-1}):** $\bar{\upsilon}$ 3749 (overtone, C=O), 3456 (stretch, OH), 3240 (stretch, OH), 3097 (stretch, CH_{Arom}), 2924 (stretch, $CH_{Aliphatic}$), 1670 (stretch, $C{=}C_{Vinyl}$), 1562 (stretch, $C{=}C_{Arom}$), 1450 (stretch, $C{=}C_{Arom}$), 1292 (stretch, OH_{phenol}), 1246 (stretch, OH_{phenol}), 1188 (stretch, C–O), 1161 (stretch, O–C), 732 (OOP, C–H); **^{1}H–NMR (300 MHz, DMSO-d_6):** δ 10.51 (s, 1H, H_{Phenol}), 8.35 (s, 1H, H_{vinyl}), 7.96 (d, J = 6.35 Hz, 1H, $H_{6'}$), 7.84–7.86 (d, J = 8.42 Hz, 2H, $H_{2',5'}$), 7.66–7.71 (t, J = 14.1 Hz, 1H, H_6), 6.90–6.93 (d, J = 8.4 Hz, 1H, H_7); **Mass (m/z, %):** 266 (M^+, 14.8), 249 (M-17, 7.4), 233 (M-33,8), 189 (M-77, 5.9), 176 (M-90, 12.5), 163 (M-103, 22.2), 152 (M-114, 19.2), 134 (M-132, 14. 8), 121 (M-145, 17), 104 (M-162, 62.9), 93 (M-173, 26.6), 76 (base peak, 100), 63 (M-203, 33.3), 50 (M-216, 74.8), 41 (M-125, 41.4).

2-(2-Hydroxy-3-methoxybenzaldehyde)-1*H*-indene-1,3(2*H*)-dione (compound 5 h)

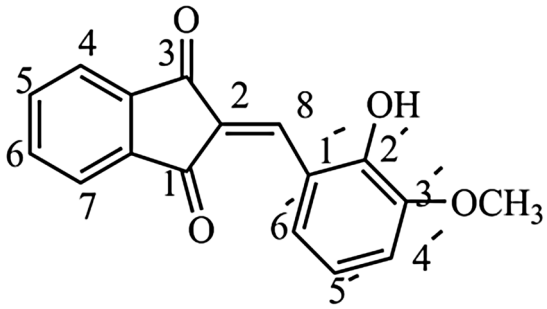

M.W. = 280.2; m.p. = 225 °C; color: Light Orange; **FT–IR (KBr, cm^{-1}):** $\bar{\upsilon}$ 3738(overtone, C=O), 3410 (stretch, OH), 3093 (stretch, CH_{Arom}), 2924 (stretch, $CH_{Aliphatic}$), 1712 (stretch, C=O), 1674 (stretch, $C{=}C_{Vinyl}$), 1577 (stretch, $C{=}C_{Arom}$), 1477 (stretch, $C{=}C_{Arom}$), 1265 (stretch, OH_{phenol}), 1215 (stretch, C–O), 1157 (stretch, $O–CH_3$), 736 (OOP, C–H); **^{1}H–NMR (300 MHz, DMSO-d_6):** δ 10.05 (s, 1H, H_{Phenol}), 8.45–8.47 (d, J = 8.15 Hz, 1H, H_4), 8.33 (s, 1H, H_{vinyl}), 7.93–7.94 (d, J = 2.75 Hz, 1H, $H_{6'}$), 7.92 (d, J = 7.95 Hz, 2H, $H_{4',5'}$), 7.90 (t, J = 2.9 Hz, 1H, H_6), 7.18–7.20 (d, J = 8 Hz, 1H, H_7), 6.86–6.89 (t, J = 16.1 Hz, 1H, H_5), 3.85 (s, 1H, $H_{Methoxy}$); **Mass (m/z, %):** 280 (M^+,11), 266 (M-14,5), 249 (M-31, 4.4), 235 (M-45, 12.5), 206 (M-74, 8), 181 (M-99, 9.6), 165 (M-115, 16.2), 152 (M-128, 38.5), 126 (M-154, 14.8), 104 (M-176, 51.8), 93 (M-187, 21.4), 76 (base peak, 100), 63 (M-217, 26.6), 50 (M-230, 54.8), 41 (M-239, 54.8).

2-(4-Hydroxy-3-methoxybenzaldehyde)-1H-indene-1,3(2H)-dione (compound 5i)

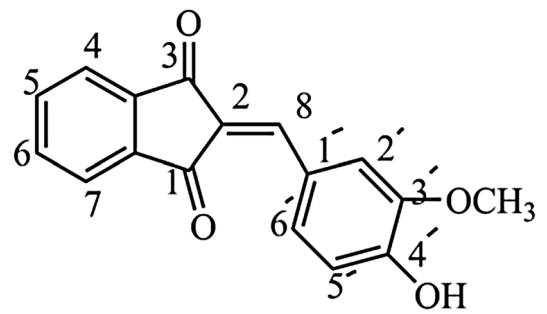

M.W. = 280.2; m.p. = 198.8 °C; color: Yellow; **FT–IR (KBr, cm^{-1}):** $\bar{\upsilon}$ 3749(overtone, C=O), 3414 (stretch, OH), 2924 (stretch, $CH_{Aliphatic}$), 1716 (stretch, C=O), 1681 (stretch, $C{=}C_{Vinyl}$), 1577 (stretch, $C{=}C_{Arom}$), 1512 (stretch, $C{=}C_{Arom}$), 1257 (stretch, OH_{phenol}), 1207 (stretch, C–O), 1157 (stretch, $O–CH_3$), 1130 (stretch, O–C), 736 (OOP, C–H); **^{1}H–NMR (300 MHz, DMSO-d_6):** δ 10.59 (s, 1H, H_{Phenol}), 8.70 (s, 1H, H_{vinyl}), 7.96–7.97 (d, J = 3.65 Hz, 1H, $H_{6'}$), 7.95 (m, 2H, $H_{2',5'}$), 7.91–7.92 (t, J = 4.2 Hz, 1H, H_6), 6.93–6.95 (d, J = 8.3 Hz, 1H, H_7), 3.92 (s, 1H, $H_{Methoxy}$); **Mass (m/z, %):** 280 (M^+, 100), 263 (M-17, 17.7), 249 (M-31, 18.5), 237 (M-43, 20.7), 209 (M-71, 13.3), 181 (M-99, 16.2), 165 (M-115, 11.8), 152 (M-128, 46.6), 133 (M-147, 8.8), 104 (M-176, 25.1), 76 (M-204, 39.2), 63 (M-217, 8), 51 (M-229, 14).

2-(4-Isopropylbenzaldehyde)-1*H*-indene-1,3(2*H*)-dione (compound 5j)

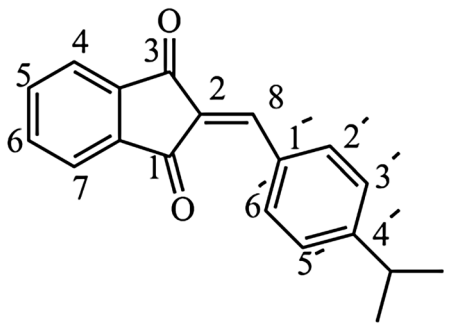

M.W. = 276.3; m.p. = 230 °C; color: Lemon**; FT–IR (KBr, cm^{-1}):** $\bar{\upsilon}$ 3506 (overtone, C=O), 3441 (stretch, OH), 3059 (stretch, CH_{Arom}), 2958 ($CH_{Aliphatic}$), 2924 (stretch, $CH_{Aliphatic}$), 1701 (stretch, C=O), 1658 (stretch, $C{=}C_{Vinyl}$), 1589 (stretch, $C{=}C_{Arom}$), 1462 (stretch, $C{=}C_{Arom}$), 1257 (stretch, OH_{phenol}), 1192 (stretch, C–O), 1157 (stretch, $O–CH_3$), 736 (OOP, C–H); **^{1}H–NMR (300 MHz, DMSO-d_6):** δ 8.64–8.66 (d, J = 7.65 Hz, 1H, H_4); **Mass (m/z, %):** 276 (M^+, 55.5), 261 (M-15, 61.4), 246 (M-30, 9.6), 233 (M-43, 100), 215 (M-61, 16.2), 202 (M-74, 17.7), 189 (M-87, 9.6), 176 (M-100, 6.6), 128 (M-148, 11.8), 115 (M-161, 13.3), 104 (M-172, 13.3), 91 (M-185, 8), 76 (M-200, 22.9), 50 (M-226, 9.6).

Formation of the FV peptide fibrils

To prepare 400 μM of the FV peptide fibrils, 2 mg of the FV peptide was dissolved in 5 ml of 50 mM phosphate buffer with pH 7, and it was well adjusted to make a clear solution, and the peptide was completely dissolved. Then it was placed at room temperature for 30–40 min to form amyloid. After this time, the solution was turbid, and amyloid was formed [17].

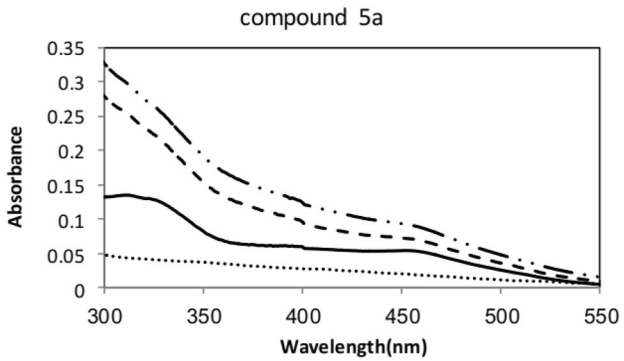

Fig. 1 Absorption spectrum of **5a** in the presence of FV peptide: compound **5a** alone (*line*), compound **5a** with peptide FV (.-.-.), subtraction of **5a** + peptide absorption spectrum from peptide (*thick dashed line*), and peptide alone (*thin dashed line*). The concentration of **5a** was 22 μM. Peptide FV concentration was 160 μM

Lysozyme formation

Four milligrams of lysozyme was weighted, and it was completely dissolved in 1 ml of 50 mM glycine with the pH 2.5. The pH of the solution was adjusted with concentrated HCl (4 M). Tube lid was covered by nylon, and the prepared solution in buffer was kept in 57 °C water bath for 72 h to aggregate lysozyme. (Increasing temperature could accelerate the process of aggregation and amyloidization.) ThT emission was measured alone and with lysozyme, at 24-h intervals, to ensure about progressing of lysozyme aggregation. Increasing ThT emission at 450 nm indicated that lysozyme was amyloidized, and increasing emission in any 24-h indicated the correct process.

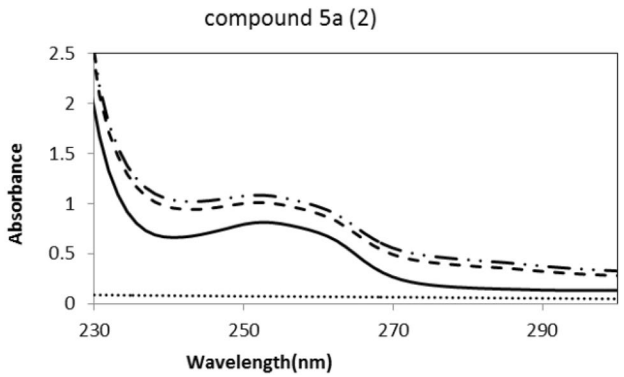

Fig. 2 Absorption spectrum of **5a** in the presence of FV peptide: compound **5a** alone (*line*), compound **5a** with peptide FV (.-.-.), subtraction of **5a** + peptide absorption spectrum from peptide (*thick dashed line*), and peptide alone (*thin dashed line*). The concentration of **5a** was 10 μM. Peptide FV concentration was 160 μM

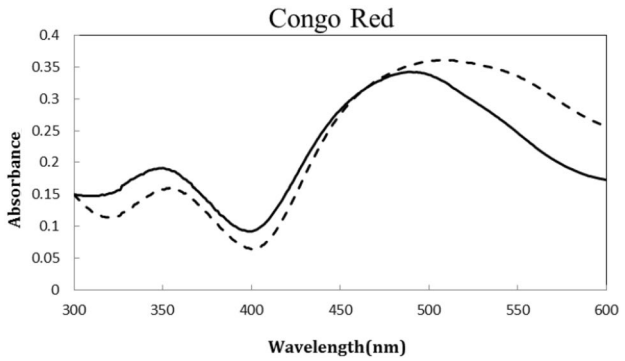

Fig. 3 CR absorption spectrum in the presence of FV peptide: CR alone (*line*), CR with peptide FV (*dashed line*). The concentration of CR was 10 μM

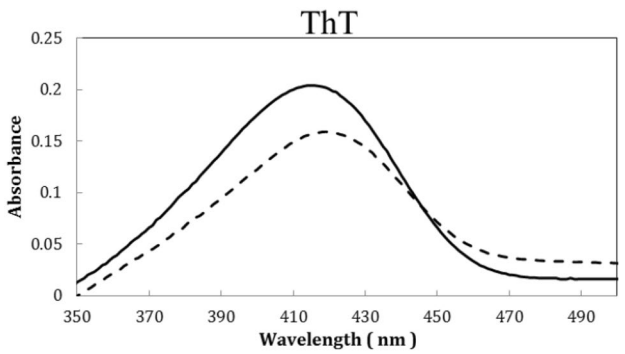

Fig. 4 ThT absorption spectrum in the presence of FV peptide: ThT alone (*line*), ThT with peptide FV (*dashed line*). The concentration of ThT was 12 μM

Preparation of beta-lactoglobulin (BLG)

0.0046 g of BLG was weighted to make a solution with a concentration of 0.5 mM, and it was dissolved in 0.5 ml of 50 mM phosphate buffer.

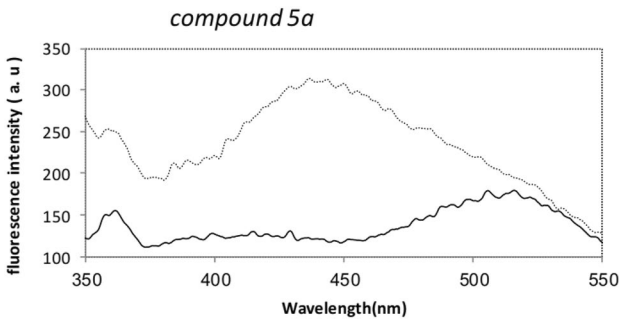

Fig. 5 Fluorescence emission spectrum of **5a** in the presence of peptide FV: **5a** alone with the concentration of 20 μM (*line*), **5a** with peptide FV with the concentration of 160 μM (*dashed line*)

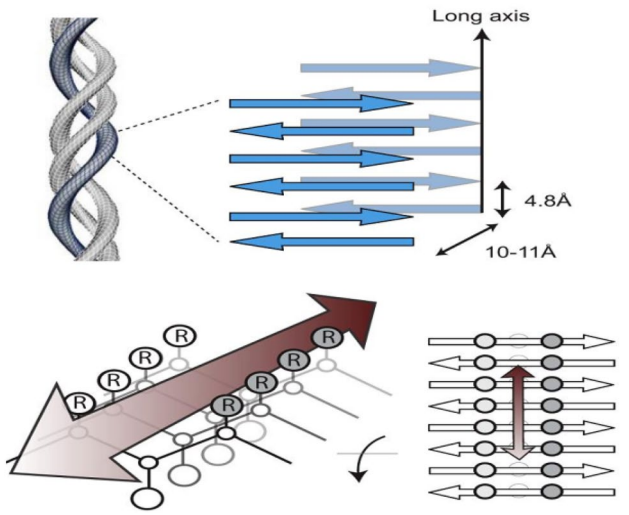

Fig. 6 The common structure of amyloid fibrils and a structural rationale for fibril–dye interactions. Top cross-β structure of amyloid fibrils, formed from layers of laminated β-sheets. Bottom "Channel" model of dye binding to fibril-like β-sheets. Dye is proposed to bind along surface side-chain grooves running parallel to the long axis of the β-sheet

Spectroscopic studies

Fluorescence excitation and emission spectra were done by Cary Eclipse fluorescence spectrophotometer (Varian, Australia). The slit width of fluorescence excitation and emission spectra was set at 5 and 10 nm. Correction of obtained spectra was performed by Cary Eclipse fluorescence spectrophotometer for the dependence of wavelength to intensity of excitation source. The main purpose of this part was to study the fluorescence reaction of each dye in the presence of native and aggregated proteins. Spectroscopic measurements were performed in standard quartz cells (1 * 1 cm). All measurements were done at room temperature. All measurements were applied at maximum excitation for each dye.

Results and discussion

A variety of 2-benzylidene-1,3-indandione derivatives **5a**–**5j** were synthesized (Table 1) and characterized with ^{1}H-NMR, FT-IR and mass spectra. For the synthetic compounds, maximum wavelengths were determined by tracking absorption spectra of the compounds, alone and in the presence of the FV peptide (all data not shown) (Figs. 1, 2), and the observed redshifts compared with CR (Fig. 3) and ThT (Fig. 4). By this way, excitation wavelengths were identified for fluorescence studies. Thereafter, formation of amyloid fibrils by the FV peptide was verified using ThT fluorescence spectroscopy as well as Congo red binding assay. The binding of all compounds to FV peptide (amyloid fibrils) shows different behavior for different compounds, unlike the ThT and compound **5a**; the fluorescence intensity of the other compounds did not show the significant increasing upon interaction with the FV peptide. According to these results, we excluded the rest of the compounds (except compound **5a**) from subsequent experiments. It is widely believed that the dramatic increase in ThT fluorescence results from the selective immobilization of ThT conformers [18, 19]. In solution, a low energy barrier allows the benzylamine and benzathiole rings of ThT to rotate freely about their shared carbon–carbon bond. This rotation rapidly quenches excited states generated by photon excitation, causing low fluorescence emission for free ThT. In contrast, rotational immobilization of ThT preserves the excited state, resulting in a high quantum yield of fluorescence [20]. In this way, there is a similar structure for Compound **5a** in which phenol ring freely rotates around the single carbon–carbon bond and quench the fluorescence emission of it, in solution. Amyloid fibrils are likely to present a binding site that

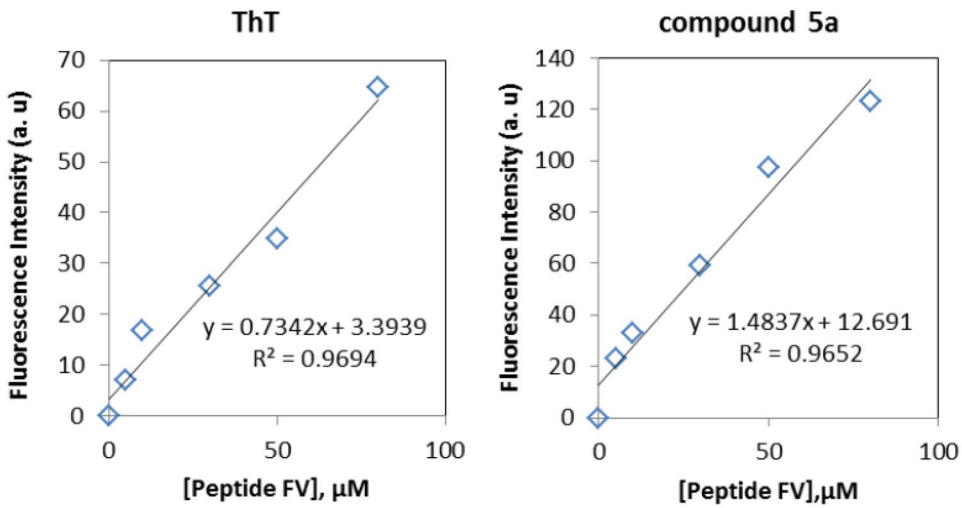

Fig. 7 Fluorescence emission spectra of **5a** and ThT in the presence of different concentrations of the FV peptide (0, 5, 10, 30, 50, 80 µM). The concentration of the compound **5a** was 20 µM

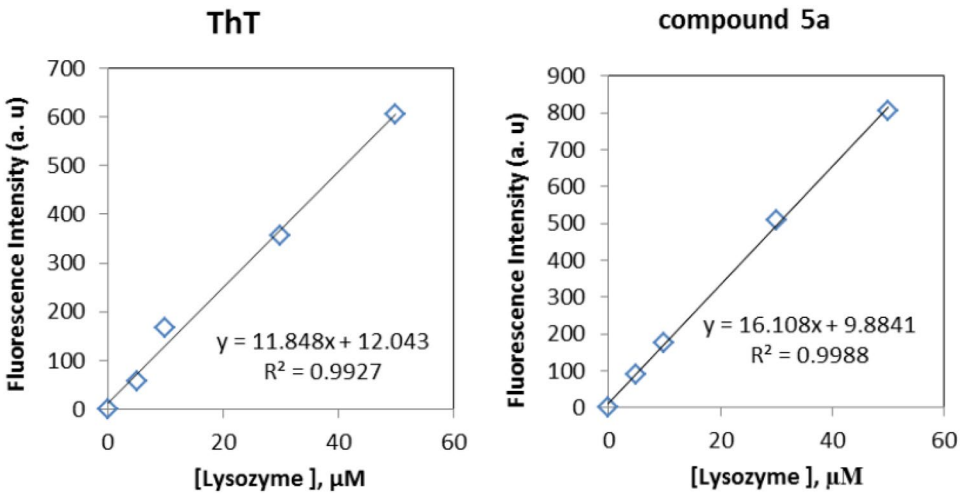

Fig. 8 Fluorescence emission spectra of **5a** and ThT in the presence of different concentrations of lysozyme (0, 5, 10, 30, 50, 80 µM). The concentration of the compound **5a** was 20 µM

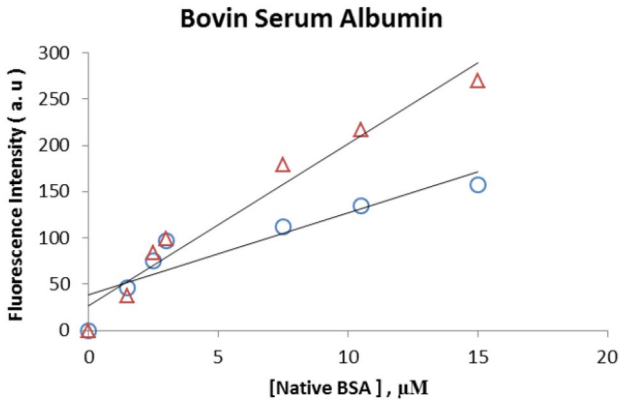

Fig. 9 Evaluation of fluorescence emission for synthesized compound **5a** after binding to native BSA at indicated concentration: The compound **5a** (Δ), Standard compound ThT (◯). The concentration of **5a** and ThT were 20 µM

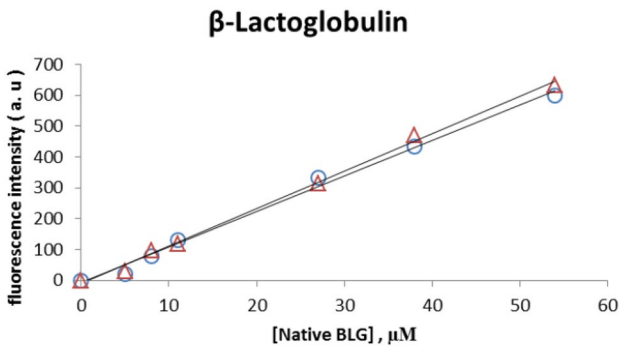

Fig. 10 Evaluation of fluorescence emission for the compound **5a** after binding to native BLG at indicated concentration: the compound **5a** (Δ), standard compound ThT (◯).The concentration of **5a** and ThT were 20 µM

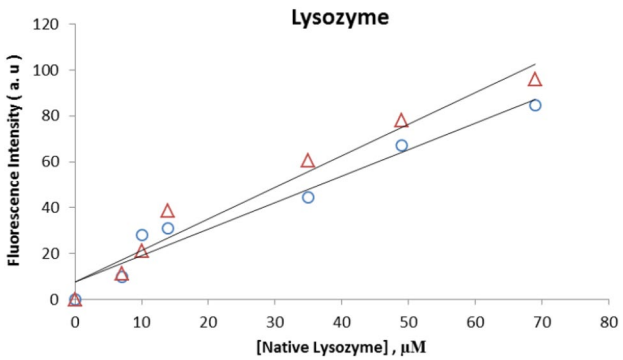

Fig. 11 Evaluation of fluorescence emission for the compound **5a** after binding to native lysozyme at indicated concentration: the compound **5a** (Δ), standard compound ThT (◯). The concentration of **5a** and ThT were 20 µM

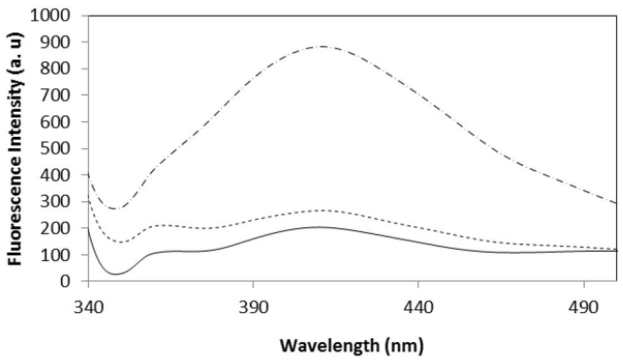

Fig. 12 Evaluation of fluorescence emission for the compound **5a** alone (*line*), with native lysozyme (*dashed line*), and amyloid lysozyme (.-.-.-). The concentration of **5a** and lysozyme were 20 µM

sterically "locks" the bound compound 5a and prevents its rotation, thus leading to an enhancement of its fluorescence.

Binding of the compound **5a** to the FV peptide was examined by observing fluorescence emission spectrum between 300 and 600 nm using specific excitation wavelengths (320 nm) and at a fixed concentration (20 μM) of compound **5a** (Fig. 5). As indicated in Fig. 5, the fluorescence intensities (emission at 440 nm) increased significantly upon interaction with amyloid aggregates.

As stated in the literature, binding of amyloid-specific dyes (such as ThT and Congo red) occurs along their long molecular axis parallel to the fibril axis [21–23]. The sequential side chains on each side of beta-sheet form "channels"—(Fig. 6), and therefore, perpendicular to the strands, it is probable that the dye molecule can insert itself into these channels. Thus, the dye molecule must be flat and thin enough to enter such a binding channel [21]. Due to the mentioned reasons, binding mechanism of dyes specific for amyloid fibrils requires further investigation.

In the next step, we measured the binding fluorescence of the compounds **5a** and ThT to the FV peptide and lysozyme aggregate, at different concentrations of the protein (0, 5, 10, 30, 50, 80 μM) (Figs. 7, 8). Moreover, as the amount of amyloid aggregates increased, the fluorescence intensities were augmented proportionally so that the maximum fluorescence emissions increased linearly as a function of amyloid concentration, in both cases. As the curve slopes indicated, the compound **5a** bind to the FV peptide and lysozyme aggregates stronger than ThT, and therefore, it is more specific for distinguishing the amyloid fibrils.

The binding fluorescence of compounds **5a** was demonstrated to be highly specific for amyloids as binding fluorescence was hardly observed with other proteins such as BSA (Fig. 9), β-LG (Fig. 10) and native lysozyme (Fig. 11) in comparison with ThT. From the curve in Fig. 12, the increase in fluorescence intensity was more significant for compound **5a** in the presence of aggregated lysozyme than native lysozyme (Fig. 12). Nevertheless, augmentation in fluorescence intensity upon binding of the compound **5a** to FV peptide and aggregated lysozyme indicated that this probe can distinguish amyloidogenic proteins from structurally unrelated proteins.

Conclusion

According to the results of this study, we have proved that our synthetic derivatives have the ability to compete with standard samples such as ThT. Due to neutrality nature of our synthetic compound **5a** and its high lipophilicity, it can be considered as a more potent probe than standard sample, ThT, for crossing blood–brain barrier.

Acknowledgements We gratefully acknowledge Vice Chancellery for Research and Technology, Kermanshah University of Medical Sciences for financial support (Grant No. 93209). This article resulted from the Pharm.D thesis of Kazhal Amiri, major of Pharmacy, Kermanshah University of Medical Sciences, Kermanshah, Iran.

References

1. G. Bhak, Y.J. Choe, S.R. Paik, BMB Rep. **42**, 541 (2009)
2. S. Babri, G. Mohaddes, I. Feizi, A. Mohammadnia, A. Niapour, A. Alihemmati et al., Eur. J. Pharmacol. **732**, 19 (2014)
3. D.R. Borchelt, T. Ratovitski, J. Van Lare, M.K. Lee, V. Gonzales, N.A. Jenkins et al., Neuron **19**, 939 (1997)
4. M. Landau, M.R. Sawaya, K.F. Faull, A. Laganowsky, L. Jiang, S.A. Sievers, J. Liu, J.R. Barrio, D. Eisenberg, PLoS Biol. **9**, e1001080 (2011)
5. B. Bulic, M. Pickhardt, B. Schmidt, E.M. Mandelkow, H. Waldmann, E. Mandelkow, Angew. Chem. Int. Ed. Engl. **48**, 1740 (2009)
6. A. Jangholi, M.R. Ashrafi-Kooshk, S.S. Arab, G. Riazi, F. Mokhtari, M. Poorebrahim, H. Mahdiuni, B.I. Kurganov, A.A. Moosavi-Movahedi, R. Khodarahmi, Archiv. Biochem. Biophys. **609**, 1 (2016)
7. W.J. Goux, L. Kopplin, A.D. Nguyen, K. Leak, M. Rutkofsky, V.D. Shanmuganandam, D. Sharma, H. Inouye, D.A. Kirschner, J. Biol. Chem. **279**, 26868 (2004)
8. N. Bijari, S. Balalaie, V. Akbari, F. Golmohammadi, S. Moradi, H. Adibi, R. Khodarahmi, Int. J. Biol. Macromol. **120**, 1009 (2018)
9. V.N. Uversky, A.L. Fink, BBA Proteins Proteom. **1698**, 131 (2004)
10. M. Biancalana, K. Makabe, A. Koide, S. Koide, J. Mol. Biol. **385**, 1052 (2009)
11. E. Voropai, M. Samtsov, K. Kaplevskii, A. Maskevich, V. Stepuro, O. Povarova et al., J Appl. Spectrosc. **70**, 868 (2003)
12. S.A. Hudson, H. Ecroyd, T.W. Kee, J.A. Carver, FEBS J. **276**, 5960 (2009)
13. M.D. Kirkitadze, A. Kowalska, Acta Biochim. Polon. **52**, 417 (2005)
14. N. Darghal, A. Garnier-Suillerot, M. Salerno, Biochem. Biophys. Res. Commun. **343**, 623 (2006)
15. S. Abbasbreigi, H. Adibi, S. Moradi, S.A. Ghadami, R. Khodarahmi, J Iran. Chem. Soc. **16**, 1225–1237 (2019)
16. S.A. Ghadami, Z. Hossein-pour, R. Khodarahmi, S. Ghobadi, H. Adibi, Med. Chem. Res. **22**, 115–126 (2013)
17. F.A. Rojas Quijano, D. Morrow, B.M. Wise, F.L. Brancia, W.J. Goux, Biochemistry **45**, 4638 (2006)
18. W. Dzwolak, M. Pecul, FEBS Lett. **579**, 6601 (2005)
19. A. Loksztejn, W. Dzwolak, J. Mol. Biol. **379**, 9 (2008)
20. M. Biancalana, S. Koide, Biochim. Biophys. Acta **1804**, 1405 (2010)
21. M.R. Krebs, E.H. Bromley, A.M. Donald, J. Struct. Biol. **149**, 30 (2005)
22. J.H. Cooper, Lab. Invest. **31**, 232 (1974)
23. L.W. Jin, K.A. Claborn, M. Kurimoto, M.A. Geday, I. Maezawa, F. Sohraby, M. Estrada, W. Kaminksy, B. Kahr, Proc. Natl. Acad. Sci. USA **100**, 15294 (2003)